Available online at www.sciencedirect.com
ScienceDirect
Ceramics International 35 (2009) 295–300
CERAMICS INTERNATIONAL
www.elsevier.com/locate/ceramint

Electrochemical properties of $LiNi_{1-y}Tl_yO_2$ cathode

MyoungYoup Song [a,*], ChanGi Park [b], Jiunn Song [c], Daniel R. Mumm [d]

[a] Division of Advanced Materials Engineering, Nanomaterials Processing Research Center, Engineering Research Institute, Chonbuk National University, 664-14 1ga Deogjindong Deogjingu, Jeonju Jeonbuk 561-756, Republic of Korea
[b] Department of Materials Engineering, Graduate School, Chonbuk National University, 664-14 1ga Deogjindong Deogjingu, Jeonju 561-756, Republic of Korea
[c] Fairmont Private Schools, Mable Campus, 1557 W. Mable Street Anaheim, CA 92802, USA
[d] Department of Chemical Engineering and Materials Science, University of California, Irvine, CA 92697-2575, USA

Received 15 May 2007; received in revised form 3 September 2007; accepted 10 October 2007
Available online 15 December 2007

Abstract

$LiNi_{1-y}Tl_yO_2$ ($y = 0.005, 0.01, 0.025, 0.05$ and 0.1) specimens were synthesized by milling and the solid-state reaction. Their electrochemical properties were compared with those of $LiNi_{1-y}M_yO_2$ (M = Ga and In). All the samples exhibited the $R\bar{3}m$ structure. $LiNi_{0.95}Tl_{0.05}O_2$ showed the largest first discharge capacity of 179.8 mAh/g and a discharge capacity of 113.8 mAh/g at the 20th cycle. $LiNi_{0.995}Tl_{0.005}O_2$ showed the smallest first discharge capacity of 125.4 mAh/g. The capacity degradation rate decreases as the discharge capacity at $n = 5$ decreases. $LiNi_{0.975}Ga_{0.025}O_2$ and $LiNi_{0.9}In_{0.1}O_2$ possessed the best electrochemical properties among the samples substituted by Ga and In, respectively. Among $LiNi_{0.975}Ga_{0.025}O_2$, $LiNi_{0.9}In_{0.1}O_2$ and $LiNi_{0.95}Tl_{0.05}O_2$, $LiNi_{0.95}Tl_{0.05}O_2$ showed the largest first discharge capacity, but the worst cycling performance. $LiNi_{0.975}Ga_{0.025}O_2$ possessed the smallest first discharge capacity, but the smallest capacity degradation rate of 0.70 mAh/(g cycle).

Keywords: $LiNi_{1-y}Tl_yO_2$; Milling; Solid-state reaction method; Electrochemical properties; I_{003}/I_{104}; *R*-factor

1. Introduction

Transition metal oxides such as $LiMn_2O_4$ [1–3], $LiCoO_2$ [4–6], and $LiNiO_2$ [7–10] have been intensively investigated in order to use them as the cathode materials of lithium secondary batteries. $LiMn_2O_4$ is comparatively inexpensive and does not bring about any environmental pollution, but its cycling performance is not adequate. $LiCoO_2$ has a large diffusivity and a high operating voltage, and it can be easily prepared. However, it has the disadvantage that it contains Co, an expensive element. $LiNiO_2$ is a very promising cathode material since it has a large discharge capacity [11] and is excellent from the economic and environmental viewpoints. On the other hand, its preparation is very difficult compared with $LiCoO_2$ and $LiMn_2O_4$.

It is known that $Li_{1-x}Ni_{1+x}O_2$ forms rather than the stoichiometric $LiNiO_2$ during preparation [12] due to cation mixing. Excess nickel occupies the Li sites, destroying the ideally layered structure and preventing the lithium ions from undergoing the easy movement required for intercalation and deintercalation during cycling. This results in a small discharge capacity and poor cycling performance.

To improve the electrochemical properties of $LiNiO_2$, Co [13], Al [14,15], Ti [16,17], Ga [11], Mn [18] and Fe [19,20] ions were substituted for nickel ions by the synthesis in oxygen. Rougier et al. [13] reported that the stabilization of the two-dimensional character of the structure by cobalt substitution in $LiNiO_2$ is correlated with an increase in the cell performance, due to the decrease in the amount of extra nickel ions in the inter-slab space which hinder the lithium diffusion. Guilmard et al. [14] investigated the electrochemical performances of $LiNi_{1-y}Al_yO_2$ ($0.10 \leq y \leq 0.50$) specimens synthesized by a co-precipitation method. They showed that aluminum substitution suppressed all the phase transitions observed for the $LiNiO_2$ system. According to Gao et al. [16], the substitution of Ti for Ni resulted in a large discharge capacity and good cycling performance. Chang et al. [17] detected partial disordering between the transition metal

* Corresponding author. Tel.: +82 63 270 2379; fax: +82 63 270 2386.
E-mail address: songmy@chonbuk.ac.kr (M. Song).

0272-8842/$34.00
doi:10.1016/j.ceramint.2007.10.016

(Ni and Ti) layer and lithium by Rietveld refinement in $Li_xNi_{1-y}Ti_yO_2$ ($0.1 \leq y \leq 0.5$) prepared by solid-state reaction. By considering the ionic radius and the Ni–O bond length, they concluded that the Ni(II) ions are partially stabilized in the lithium sites. Nishida et al. [11] reported that gallium-doping into $LiNiO_2$ stabilizes the crystal structure during the charging process and leads to better cycling performance than $LiNiO_2$. Guilmard et al. [18] reported the presence of 5 and 3% extra nickel ions in the inter-slab space in two types of $LiNi_{0.90}Mn_{0.10}O_2$ synthesized by a co-precipitation method in the presence of 5 and 50% lithium excesses, respectively. The cycling test showed a worsening in the electrochemical properties with a large irreversible capacity at the end of the first cycle compared with $LiNiO_2$. Reimers et al. [19] studied a solid solution series of $LiFe_yNi_{1-y}O_2$ ($0.1 \leq y \leq 0.5$). They reported that the cation mixing was primarily between Fe and Li, and that the amount of Li which can be reversibly cycled decreases as y increases. Kanno et al. [20] synthesized $LiFe_{1-y}Ni_yO_2$ by the ion-exchange reaction and reported that the cycling capacities of the 4 V region decreased with increasing iron content.

In this work, $LiNi_{1-y}Tl_yO_2$ ($y = 0.005$, 0.01, 0.025, 0.05 and 0.1) specimens were synthesized by milling and solid-state reaction, and the electrochemical properties of the synthesized samples were investigated. Their electrochemical properties were then compared with those of $LiNi_{1-y}M_yO_2$ (M = Ga and In) specimens synthesized by the same method in our previous work [21,22].

2. Materials and methods

The $LiNi_{1-y}Tl_yO_2$ ($y = 0.005$, 0.01, 0.025, 0.05 and 0.1) specimens were synthesized by milling and solid-state reaction under the optimum conditions for the preparation of $LiNiO_2$, as previously reported [23]. $LiOH{\cdot}H_2O$ (Kojundo Chemical Lab. Co. Ltd., purity 99%), $Ni(OH)_2$ (Kojundo Chemical Lab. Co. Ltd., purity 99.9%), and $TlNO_3$ (Aldrich Chemical, 99.9%) were used as the starting materials. These were mechanically mixed by SPEX milling for 1 h, then preheated at 450 °C for 5 h in air, pressed into pellets and calcined at 750 °C for 30 h under an oxygen stream. The phase identification of the synthesized samples was carried out by the X-ray powder diffraction analysis (Rigaku III/A diffractometer) using Cu Kα radiation, scanning rate of $6^\circ\ min^{-1}$ and 2θ of $10^\circ \leq 2\theta \leq 80^\circ$. The electrochemical cells consisted of $LiNi_{1-y}Tl_yO_2$ as a positive electrode, Li foil as a negative electrode and an electrolyte [Purelyte (Samsung General Chemicals Co. Ltd.)] prepared by dissolving 1 M $LiPF_6$ in a 1:1 (volume ratio) mixture of ethylene carbonate (EC) and diethyl carbonate (DEC). The positive electrode consisted of 85 wt.% synthesized materials, 10 wt.% acetylene black and 5 wt.% polyvinylidene fluoride (PVDF) binder dissolved in 1-methyl-2-pyrrolidinone (NMP). A Whatman glass-filter was used as a separator. The coin-type (2016) cells were assembled in an argon-filled dry box. All of the electrochemical tests were performed at room temperature with a potentiostatic/galvanostatic system. The cells were cycled between 2.7 and 4.2 V at a rate of 0.1 C.

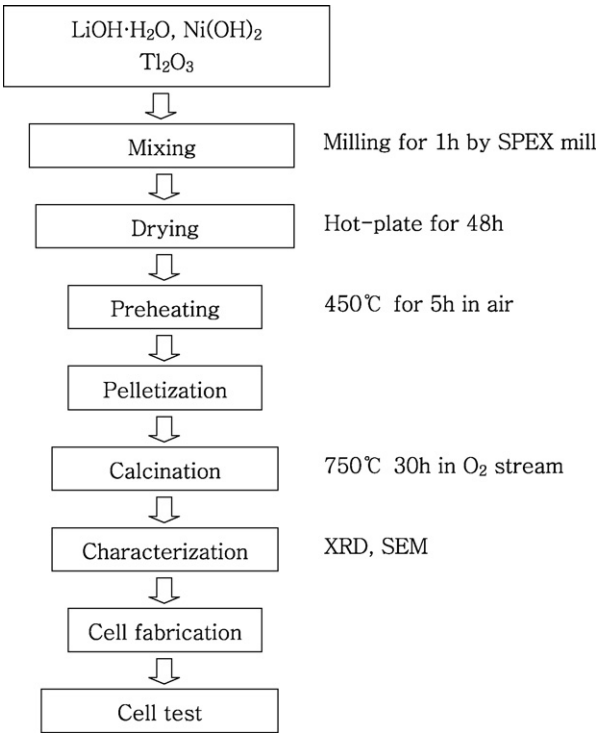

Fig. 1. Experimental procedure for $LiNi_{1-y}Tl_yO_2$ electrode prepared by the solid-state reaction method after milling.

Fig. 1 shows the experimental procedure for the $LiNi_{1-y}Tl_yO_2$ electrodes prepared by the solid-state reaction method after milling.

3. Results and discussion

Fig. 2 shows the X-ray powder diffraction (XRD) patterns of the $LiNi_{1-y}Tl_yO_2$ ($y = 0.005$, 0.01, 0.025, 0.05 and 0.01) specimens calcined at 750 °C for 30 h. All the samples possess the α-$NaFeO_2$ structure of the rhombohedral system (space group: $R\bar{3}m$) with no evidence of any impurities. The $R\bar{3}m$ structure is distorted in the c-axis direction of the hexagonal structure. This is reflected by the split of the 0 0 6 and 1 0 2

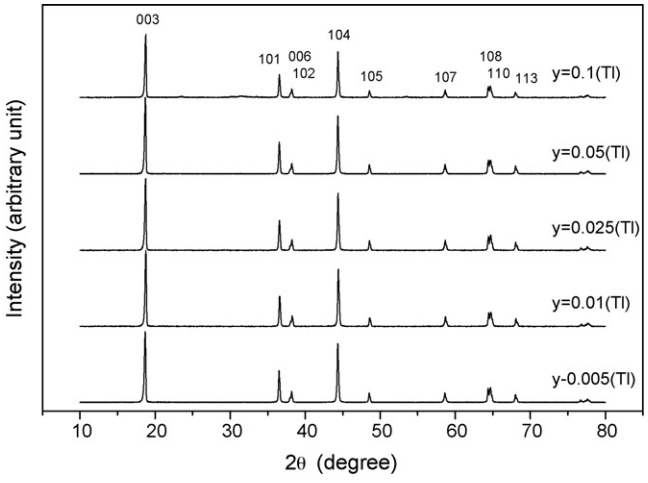

Fig. 2. XRD patterns of $LiNi_{1-y}Tl_yO_2$ ($y = 0.005$, 0.01, 0.025, 0.05 and 0.1) calcined at 750 °C for 30 h.

Table 1
Data calculated from XRD patterns of $LiNi_{1-y}Tl_yO_2$ ($y = 0.005$, 0.01, 0.025, 0.05 and 0.1) calcined at 750 °C for 30 h

	a(Å)	c(Å)	I_{003}/I_{104}	R-factor	Unit cell volume (Å^3)
$y = 0.1$	2.786	14.178	1.02	0.59	101.872
$y = 0.05$	2.880	14.223	1.12	0.53	101.320
$y = 0.025$	2.877	14.195	1.05	0.56	102.240
$y = 0.01$	2.877	14.207	0.98	0.52	101.843
$y = 0.005$	2.882	14.239	1.16	0.50	102.108

peaks and of the 1 0 8 and 1 1 0 peaks in the XRD patterns. The 1 0 8 and 1 1 0 peaks were split for all of the samples.

Ohzuku et al. [24] reported that electrochemically reactive $LiNiO_2$ showed a larger integrated intensity ratio of the 0 0 3 peak to the 1 0 4 peak (I_{003}/I_{104}) and a clear split of the 1 0 8 and 1 1 0 peaks in its XRD patterns. The degree of cation mixing (displacement of nickel and lithium ions) is low if the value of I_{003}/I_{104} is large and the 1 0 8 and 1 1 0 peaks are split clearly. The value of $(I_{006} + I_{102})/I_{101}$, called the R-factor, is known to decrease as the unit cell volume of $Li_yNi_{2-y}O_2$ decreases. The R-factor increases as y in $Li_yNi_{2-y}O_2$ decreases for y near 1. This indicates that the R-factor increases as the degree of cation mixing becomes larger [7].

Table 1 gives the lattice parameters, a, c, c/a, I_{003}/I_{104}, R-factor and unit cell volume calculated from the XRD patterns of $LiNi_{1-y}Tl_yO_2$ ($y = 0.005$, 0.01, 0.025, 0.05 and 0.01) calcined at 750 °C for 30 h. The sample with $y = 0.005$ has the largest value of I_{003}/I_{104} and the smallest value of the R-factor among all of the samples.

Fig. 3 shows SEM micrographs of $LiNi_{1-y}Tl_yO_2$ ($y = 0.005$, 0.01, 0.025, 0.05 and 0.01) calcined at 750 °C for 30 h. The samples contain small and large particles. The particles become larger as the value of y increases.

Fig. 4 shows the variations of the discharge capacity of $LiNi_{1-y}Tl_yO_2$ ($y = 0.005$, 0.01, 0.025, 0.05 and 0.01) calcined at 750 °C for 30 h. The sample with $y = 0.05$ has the largest first discharge capacity of 179.8 mAh/g and a discharge capacity of 113.8 mAh/g at the 20th cycle. The sample with $y = 0.005$ has the smallest first discharge capacity of 125.4 mAh/g.

Fig. 5 shows the variation of the capacity degradation rate between $n = 5$ and 20 with the discharge capacity at $n = 5$ for $LiNi_{1-y}Tl_yO_2$ ($y = 0.005$, 0.01, 0.025, 0.05 and 0.1) calcined at

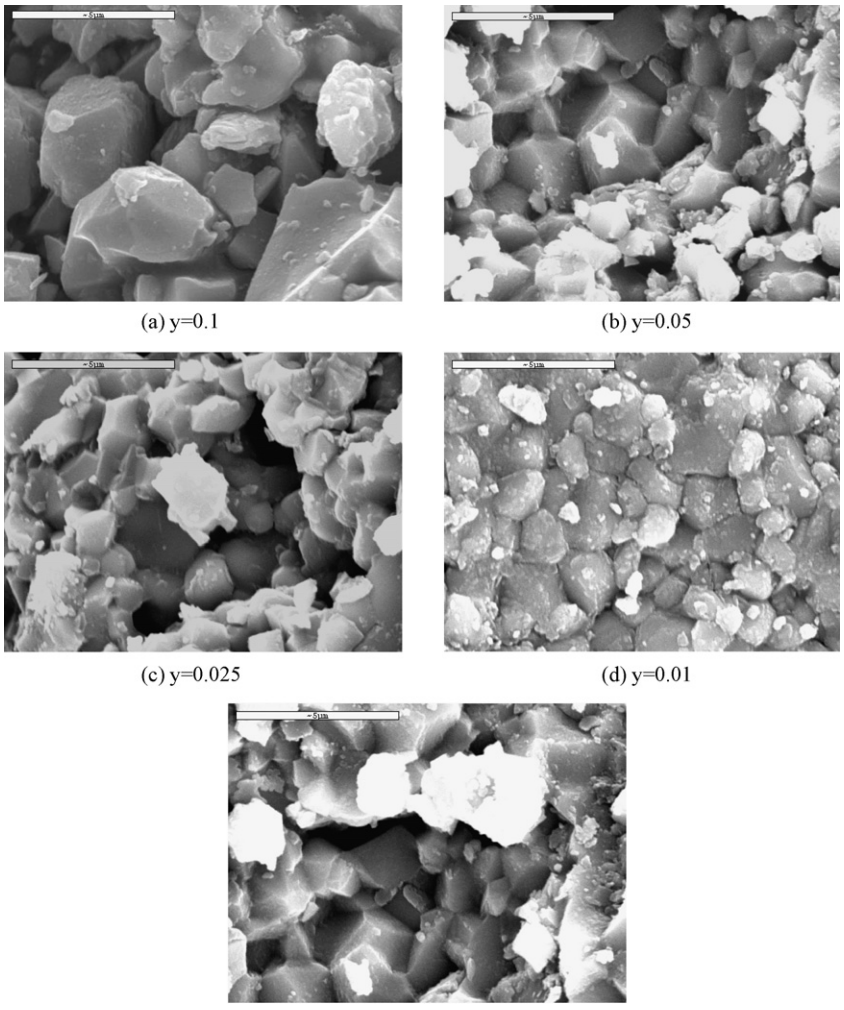

Fig. 3. SEM micrographs of $LiNi_{1-y}Tl_yO_2$ ($y = 0.005$, 0.01, 0.025, 0.05 and 0.1) calcined at 750 °C for 30 h.

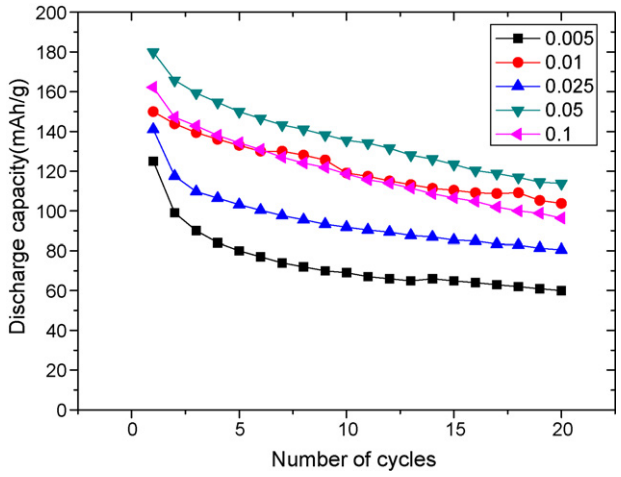

Fig. 4. Variations of discharge capacity at 0.1 C-rate with the number of cycles for $LiNi_{1-y}Tl_yO_2$ (y = 0.005, 0.01, 0.025, 0.05 and 0.1) calcined at 750 °C for 30 h.

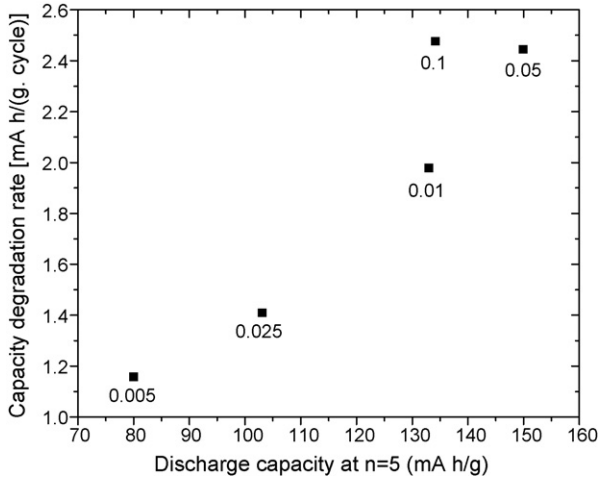

Fig. 5. Variation of the capacity degradation rate between n = 5 and 20 with the discharge capacity at n = 5 for $LiNi_{1-y}Tl_yO_2$ (y = 0.005, 0.01, 0.025, 0.05 and 0.1) calcined at 750 °C for 30 h.

750 °C for 30 h. The capacity degradation rates were calculated from the discharge capacities between the 5th and the 20th discharge cycles. This range of n is chosen because the discharge capacity varies steadily after n = 5. The capacity degradation rate decreases as the discharge capacity at n = 5 decreases. The expansion and contraction of $LiNi_{1-y}Tl_yO_2$ due to intercalation and deintercalation causes the unit cell to become strained and distorted. The interstitial sites and thus, the structure will be more severely destroyed when the electrode is cycled at a larger value of Δx in $Li_xNi_{1-y}Tl_yO_2$. A larger Δx, to which the discharge capacity is proportional, is considered to bring about a larger capacity degradation rate with cycling.

In our previous works [21,22], we studied the electrochemical properties of $LiNi_{1-y}Ga_yO_2$ and $LiNi_{1-y}In_yO_2$ synthesized by the same method, as mentioned above. Among the various $LiNi_{1-y}Ga_yO_2$ specimens, $LiNI_{0.975}Ga_{0.025}O_2$ had the best electrochemical properties, while $LiNi_{0.9}In_{0.1}O_2$ exhibited the best electrochemical properties among the various $LiNi_{1-y}In_yO_2$ samples.

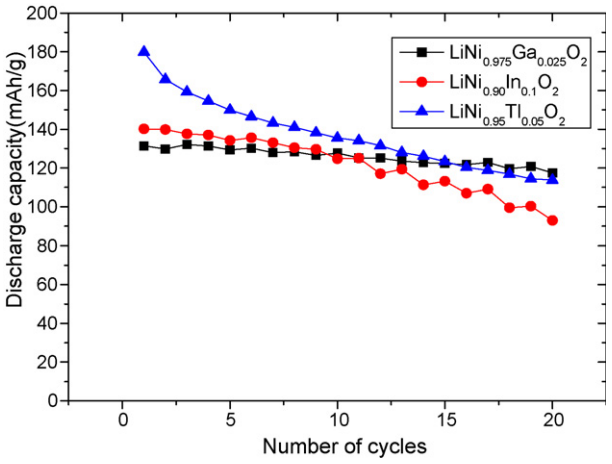

Fig. 6. Variations of discharge capacity at 0.1 C-rate with the number of cycles for $LiNi_{1-y}M_yO_2$ (M = Ga, y = 0.025; M = In, y = 0.1; M = Tl, y = 0.05) calcined at 750 °C for 30 h.

Fig. 6 shows the variations of the discharge capacity of $LiNi_{1-y}M_yO_2$ (M = Ga, y = 0.025; M = In, y = 0.1; M = Tl, y = 0.05) calcined at 750 °C for 30 h. The sample $LiNi_{0.95}Tl_{0.05}O_2$ had the largest first discharge capacity of 179.8 mAh/g and a discharge capacity of 113.8 mAh/g at the 20th cycle. The sample $LiNi_{0.975}Ga_{0.025}O_2$ had the smallest first discharge capacity of 131.4 mAh/g, but it has the best cycling performance. $LiNi_{0.975}Ga_{0.025}O_2$ has a discharge capacity of 117.5 mAh/g at the 20th cycle, showing a discharge capacity degradation rate of 0.70 mAh/(g cycle).

Fig. 7 shows the XRD patterns of $LiNi_{0.975}Ga_{0.025}O_2$, $LiNi_{0.9}In_{0.1}O_2$ and $LiNi_{0.95}Tl_{0.05}O_2$. All of the samples have the phase with the $R\bar{3}m$ structure. In addition, the XRD pattern of $LiNi_{0.9}In_{0.1}O_2$ shows peaks corresponding to $LiInO_2$.

Table 2 gives the lattice parameters a, c, c/a, I_{003}/I_{104}, R-factor and unit cell volume calculated from the XRD patterns of $LiNi_{1-y}M_yO_2$ (M = Ga, y = 0.025; M = In, y = 0.1; M = Tl, y = 0.05). $LiNi_{0.9}In_{0.1}O_2$ has the largest value of I_{003}/I_{104} and all of the samples have similar values of the R-factor.

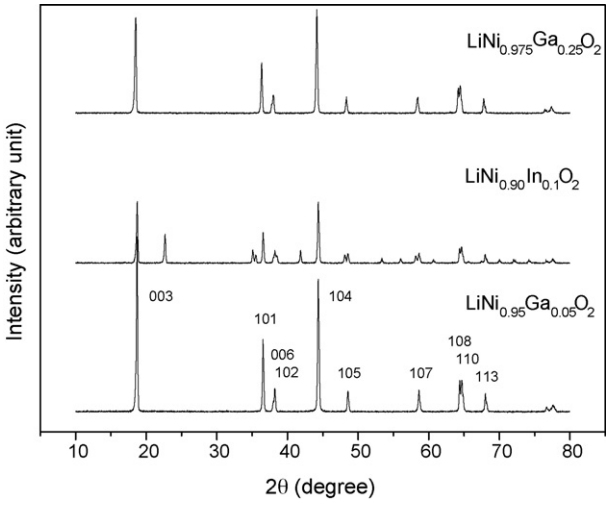

Fig. 7. X-ray powder diffraction patterns of $LiNi_{1-y}M_yO_2$ (M = Ga, y = 0.025; M = In, y = 0.1; M = Tl, y = 0.05) calcined at 750 °C for 30 h.

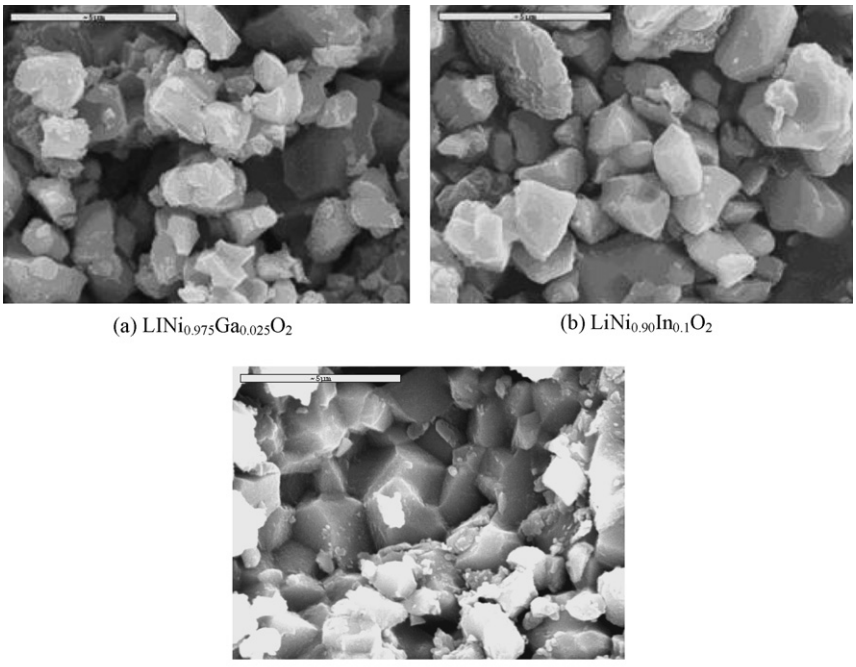

(a) $LINi_{0.975}Ga_{0.025}O_2$ (b) $LiNi_{0.90}In_{0.1}O_2$

(c) $LiNi_{0.95}Tl_{0.05}O_2$

Fig. 8. SEM micrographs of $LiNi_{1-y}M_yO_2$ (M = Ga, $y = 0.025$; M = In, $y = 0.1$; M = Tl, $y = 0.05$) calcined at 750 °C for 30 h.

Table 2
Data calculated from X-ray powder diffraction patterns of $LiNi_{1-y}M_yO_2$ (M = Ga, $y = 0.025$; M = In, $y = 0.1$; M = Tl, $y = 0.05$) calcined at 750 °C for 30 h

	a(Å)	c(Å)	I_{003}/I_{104}	R-factor	Unit cell volume (Å^3)
$LiNi_{0.975}Ga_{0.025}O_2$	2.883	14.362	0.92	0.54	103.380
$LiNi_{0.90}In_{0.1}O_2$	2.877	14.212	1.33	0.52	101.559
$LiNi_{0.95}Tl_{0.05}O_2$	2.880	14.223	1.12	0.53	101.320

Fig. 8 shows SEM micrographs of $LiNi_{0.975}Ga_{0.025}O_2$, $LiNi_{0.9}In_{0.1}O_2$ and $LiNi_{0.95}Tl_{0.05}O_2$ calcined at 750 °C for 30 h. All of the samples contain both small and large particles. The particle size increases roughly in the order from $LiNI_{0.975}Ga_{0.025}O_2$ to $LiNi_{0.9}In_{0.1}O_2$ and then to $LiNi_{0.95}Tl_{0.05}O_2$. The particles of $LiNi_{0.95}Tl_{0.05}O_2$ are agglomerated.

4. Conclusions

$LiNi_{1-y}Tl_yO_2$ ($y = 0.005$, 0.01, 0.025, 0.05 and 0.1) specimens were synthesized by milling for 1 h, preheating at 450 °C for 5 h in air, then pelletizing, and finally calcining at 750 °C for 30 h under an oxygen stream. All of the samples had the $R\bar{3}m$ structure. $LiNi_{0.95}Tl_{0.05}O_2$ had the largest first discharge capacity of 179.8 mAh/g and a discharge capacity of 113.8 mAh/g at the 20th cycle. $LiNi_{0.995}Tl_{0.005}O_2$ had the smallest first discharge capacity of 125.4 mAh/g. The capacity degradation rate decreases as the discharge capacity at $n = 5$ decreases. $LiNi_{0.975}Ga_{0.025}O_2$ and $LiNi_{0.9}In_{0.1}O_2$ had the best electrochemical properties among the samples substituted by Ga and In, respectively. Among $LiNi_{0.975}Ga_{0.025}O_2$, $LiNi_{0.9}In_{0.1}O_2$ and $LiNi_{0.95}Tl_{0.05}O_2$, $LiNi_{0.95}Tl_{0.05}O_2$ had the largest first discharge capacity, but the worst cycling performance. $LiNi_{0.975}Ga_{0.025}O_2$ had the smallest discharge capacity, but the smallest capacity degradation rate of 0.70 mAh/(g cycle).

Acknowledgement

This work was supported by Grant No. R01-2003-000-10325-0 from the Basic Research Program of the Korea Science & Engineering Foundation.

References

[1] J.M. Tarascon, E. Wang, F.K. Shokoohi, W.R. McKinnon, S. Colson, J. Electrochem. Soc. 138 (1991) 2859.
[2] A.R. Armstrong, P.G. Bruce, Lett. Nat. 381 (1996) 499.
[3] M.Y. Song, D.S. Ahn, Solid State Ionics 112 (1998) 245.
[4] K. Ozawa, Solid State Ionics 69 (1994) 212.
[5] R. Alcántara, P. Lavela, J.L. Tirado, R. Stoyanova, E. Zhecheva, J. Solid State Chem. 134 (1997) 265.
[6] Z.S. Peng, C.R. Wan, C.Y. Jiang, J. Power Sources 72 (1998) 215.
[7] J.R. Dahn, U. von Sacken, C.A. Michal, Solid State Ionics 44 (1990) 87.
[8] J.R. Dahn, U. von Sacken, M.R. Jukow, H. Aljanaby, J. Electrochem. Soc. 138 (1991) 2207.
[9] A. Marini, V. Massarotti, V. Berbenni, D. Capsoni, R. Riccardi, E. Antolini, B. Passalacqua, Solid State Ionics 45 (1991) 143.
[10] W. Ebner, D. Fouchard, L. Xie, Solid State Ionics 69 (1994) 238.
[11] Y. Nishida, K. Nakane, T. Stoh, J. Power Sources 68 (1997) 561.
[12] J. Morales, C. Perez-Vicente, J.L. Tirado, Mater. Res. Bull. 25 (1990) 623.
[13] A. Rougier, I. Saadoune, P. Gravereau, P. Willmann, C. Delmas, Solid State Ionics 90 (1996) 83.
[14] M. Guilmard, A. Rougier, M. Grune, L. Croguennec, C. Delmas, J. Power Sources 115 (2003) 305.
[15] M.Y. Song, R. Lee, I.H. Kwon, Solid State Ionics 156 (2003) 319.
[16] Y. Gao, M.V. Yakovleva, W.B. Ebner, Electrochem. and Solid-State Lett. 1 (1998) 117.

[17] S.H. Chang, S.G. Kang, S.W. Song, J.B. Yoon, J.H. Choy, Solid State Ionics 86–88 (1996) 171.
[18] M. Guilmard, L. Croguennec, C. Delmas, J. Electrochem. Soc. 150 (10) (2003) A1287.
[19] J.N. Reimers, E. Rossen, C.D. Jones, J.R. Dahn, Solid State Ionics 61 (1993) 335.
[20] R. Kanno, T. Shirane, Y. Inaba, Y. Kawamoto, J. Power Sources 68 (1997) 145.
[21] H.U. Kim, S.D. Youn, J.C. Lee, H.R. Park, C.G. Park, M.Y. Song, J. Korean Ceram. Soc. 42 (9) (2005) 631.
[22] H.U. Kim, S.D. Youn, J.C. Lee, H.R. Park, C.G. Park, M.Y. Song, Trans. Korean Hydrogen New Energy Soc. 16 (4) (2005) 385.
[23] H.U. Kim, S.D. Youn, J.C. Lee, H.R. Park, M.Y. Song, J. Korean Ceram. Soc. 42 (5) (2005) 319.
[24] T. Ohzuku, A. Ueda, M. Nagayana, J. Electrochem. Soc. 140 (1993) 1862.